Journal of Hazardous Materials 199–200 (2012) 272–281

Contents lists available at SciVerse ScienceDirect

Journal of Hazardous Materials

journal homepage: www.elsevier.com/locate/jhazmat

Research on soot of black smoke from ceramic furnace flue gas: Characterization of soot

Pei Lu[a,b], Caiting Li[a,b,*], Guangming Zeng[a,b], Xuwen Xie[a,b], Zhihong Cai[a,b], Yangxin Zhou[a,b], Yapei Zhao[a,b], Qi Zhan[a,b], Zheng Zeng[a,b]

[a] College of Environmental Science and Engineering, Hunan University, Changsha 410082, China
[b] Key Laboratory of Environmental Biology and Pollution Control (Hunan University), Ministry of Education, Changsha 410082, China

ARTICLE INFO

Article history:
Received 12 June 2011
Received in revised form 1 November 2011
Accepted 3 November 2011
Available online 9 November 2011

Keywords:
Soot
Nanoparticle
Organic compounds
Hazardous materials

ABSTRACT

In this study, the characterizations of soot from ceramic furnace flue gas were studied using environmental scanning electron microscopy, energy dispersive spectroscopy, particle size distribution, specific surface area measurements, crystal characterizations and organic pollutant analysis. Soot particles were mainly spherical nanoparticles with diameters less than 100 nm. However, the particles could be aggregated into larger ones with a median diameter of 3.66 μm. Nanometer pores with diameters ranging 2–4 nm were also detected in the soot particles. Because of their large surface areas and pore volumes, other pollutants in the environment can be adsorbed to soot particles potentially making them more hazardous. Several elements, including C, O and Pb, were detected in the soot, but only small amounts of crystalline materials were observed. This is because most of the detected carbon and metals/metal oxides/metal salts were amorphous. Approximately 90 different organic pollutants were detected in the soot, including aromatic compounds and other hydrocarbons. Because of the carcinogenic properties of aromatic compounds and the photochemical effects of hydrocarbons, soot could have serious health and environmental impacts. The results suggest that soot particles are hazardous material and urgently need to be controlled.

1. Introduction

Atmospheric aerosols are the major air pollutants and have global and local environmental impacts [1,2]. They can affect the climate directly through the scattering and absorption of incoming solar radiation [3–5], and can result in environmental pollution [6] that causes serious health problems [7,8]. Soot in black smoke (BS) is the result of incomplete combustion of carbon-based fuels, like fossil and bio-fuels [9,10], and is a significant anthropogenic aerosol source [11]. However, it is disappointing that soot in many countries, especially developing countries like China [6], has not been effectively controlled [12].

Since soot particles originate from the incomplete combustion of carbonaceous materials, soot emissions are mainly from biomass burning, the combustion of coal and the consumption of fuel by industrial processes [13–15]. Meanwhile, when soot is emitted into environment, because of its small particle sizes [2,13,16], large specific surface area [17] and long atmospheric lifetime (from several days to weeks) [16], it will adsorb other air pollutants. These pollutants include heavy metals like Pb, Hg and Cd [16], heavy metal compounds, like MNO_3 and MSO_4 [18], and organic pollutants like polycyclic aromatic hydrocarbons (PAHs) and volatile organic compounds [19,20]. Because of its adsorption properties, soot in atmosphere could have increased negative impacts on climate [21], the environment and human health. It has been reported that increased rainfall in south China, severe drought in north China over the past several decades and increased incidences of cancer are the result of soot pollution [11,22–24].

Because soot is both a local and a global pollutant, the research on soot has become a hot topic in recent years [11,16,25]. Meanwhile, the carbon based fuels are still widely used for industrial and domestic combustion in developing countries, resulting in serious particulate matter and other air pollutions [26]. In order to efficiently reduce soot emission, it would be desirable for soot to be removed using surfactant solutions before it is emitted into atmosphere. This is particularly important for soot emitted from coal or oil-fired boiler and kiln [17]. To effectively remove soot from emissions, the characterizations of soot should be primarily and completely studied. However, many of the previous reports were mainly focused on the collection and analysis of soot [23,27] or the simulated distribution of soot particles [14,25,26,28]. The

* Corresponding author at: College of Environmental Science and Engineering, Hunan University, Changsha 410082, China. Tel.: +86 731 88649216; fax: +86 731 88649216.
E-mail addresses: lupei@hnu.edu.cn, hdlupei@163.com (P. Lu), ctli@hnu.edu.cn, ctli3@yahoo.com (C. Li).

0304-3894/$ – see front matter © 2011 Elsevier B.V. All rights reserved.
doi:10.1016/j.jhazmat.2011.11.004

characterizations of soot particles have rarely been researched. Up to now, the most effective way to reduce soot pollution is to remove the soot from the BS of flue gas. The removal method used is highly dependent on the characterizations of the soot. In this study, basic but very important characteristics of soot, such as surface features, particle size distributions and chemical content were specially studied. The results of this study provide useful information for follow-up experimental studies on the health effects of soot and potential removal methods. The results should also allow for the application of efficient controls on soot emissions from BS before reaching the atmosphere.

2. Experimental methods and instrumentation

2.1. Samples

Soot samples for this study were collected from a coal-fired ceramics factory in Liling, Zhuzhou, Hunan Province, China. The coal used was anthracite and was supplied by Hunan Baisha Coal and Electricity Group of China. The coal was combusted at 1100 °C. Samples were collected from the chimney exhaust port using a dust sampler (TH 880F, Wuhan Tianhong Co., Ltd., China) with ultra-fine glass fiber non-gel filter cartridges (Shandong Tengxiang Glass Fiber Reinforced Plastic Group, China). Samples were collected for 5 min three times per hour for 10 h during 1 day. The sampling gas flow rate was 35 L/min with a precision of 0.1 L/min. The sampling efficiency of the ultra-fine glass fiber non-gel filter cartridge was 99.9999% when particle sizes were larger than 0.3 μm and the work temperature was below 600 °C. Upon collection, all of the samples were mixed and stored in sealed bags to prevent them from being polluted. Once returned to the laboratory, the samples were dried in oven (DHG-9023A, Shanghai Qin Mai Instrument Co., Ltd.) at 80 °C and stored in clean, sealed bags until analysis.

2.2. Experimental methods

Soot particle size distributions were analyzed by a laser particle size analyzer (BT-9300H, Dandong Baite Instrument Co., Ltd.). Dispersant was not used for this experiment. The specific surface areas of the soot samples were calculated using N_2 adsorption isotherms by applying the Brunauer–Emmett–Teller (BET) equation, which yielded important information about the particle size distributions of soot (3100, Beckman Coulter, USA) [29].

Surface characteristics of the samples and their elemental compositions were studied using environmental scanning electron microscopy (ESEM) and energy dispersive spectroscopy (EDS) (QUANTA 200, FEI Co. Ltd., USA), respectively.

Powder X-ray diffraction (XRD) measurements were carried out using a Rigaku Rotaflex D/Max-C system with Cu Kr (λ = 0.1543 nm) radiation (D5000, Siemens Co., Germany). The samples were loaded into a sample holder with a depth of 1 mm. The diffraction angle 2θ was between 10° and 40°. The X-ray gun operating voltage was 35 kV. The tube current and scanning speed were 30 mA and 2°/min, respectively.

Particulate matter samples were extracted twice in an ultrasonic bath (SB, model 3200) with 30 mL dichloromethane for 30 min. The extracts were combined and concentrated to 1 mL using a stream of nitrogen. The concentrated extracts were purified and fractionated using column chromatography. The column was packed using 15 cm of silica gel 100–200 (Merck, Qingdao; activated at 105 °C for 24 h) and 1 cm of anhydrous sodium sulfate (baked at 600 °C for 6 h) as slurries in dichloromethane, respectively. Hexane (40 mL) was used to rinse the column. The extract was applied to the top of the column and eluted with 25 mL hexane and 25 mL hexane–dichloromethane (v:v = 1:1). The collected fractions were concentrated to 1 mL using a rotary evaporator, transferred to a 2 mL vial and preserved in a freezer at −18 °C until analysis using gas chromatography–mass spectrometry (GC/MS) (Thermo-Finnigan, Polaris Q, Thermo Fisher Scientific, USA) [20].

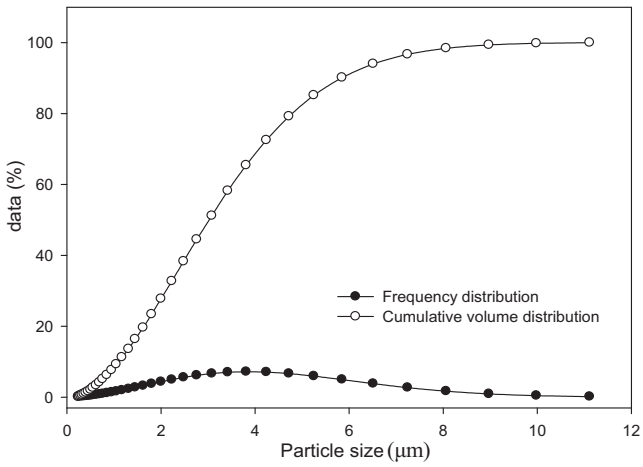

Fig. 1. Soot particle size distribution.

Organic compounds in the soot samples were identified using GC/MS. Selected ion monitoring was used as the detection mode for organic compound identification. The GC was equipped with a DB-5 MS capillary column (30 m × 0.25 mm inner diameter, film thickness 0.25 μm) and high-purity helium was used as the carrier gas. The oven temperature program was programmed as follows. The temperature was held at 60 °C for 5 min, increased to 160 °C at a rate of 10 °C/min, increased to 240 °C at a rate of 15 °C/min and finally held at 300 °C for 20 min. The injector and detector temperatures were 280 °C and 300 °C, respectively. During each run, 1 μl of sample was injected in the splitless mode [20].

3. Results and discussion

3.1. Particle size distributions

Particle size is probably the most important single physical characteristic. The Rosin–Rammler (R–R) distribution function has long been used to describe particle size distributions. The general expression of the R–R distribution function is [31]:

$$log\left(\ln\left(\frac{1}{1-G}\right)\right) = \log\left(\frac{1}{\bar{d}_p^n}\right) + n\ \log\ d_p \quad (1)$$

where G is the percentage, by mass, of particles larger than the screen size, d_p; $\bar{d}_p$ is the equivalent mean size when $G = 63.2\%$; and n is the distribution exponent [31,32].

To obtain the raw particle size distribution of soot, particle size distribution experiments were carried out using a laser particle size analyzer without dispersant. Fig. 1 shows the particle size distribution of soot. When the results shown in Fig. 1 were treated by R–R distribution function, the particle distribution was found to be consistent with the R–R distribution. It is shown in Fig. 2.

According to Fig. 1 and the regression equation, shown as Eq. (2), the median diameter of the soot particles was 3.66 μm and the distribution index was 2.021.

$$\bar{d}_p = \exp\left(-\left(\frac{d_p}{3.66}\right)^{2.021}\right) \quad (2)$$

From Fig. 1 it was illustrated that soot particle sizes were largely distributed between 1 μm and 8 μm, with most particles between 1 μm and 2 μm. The soot particle diameters determined

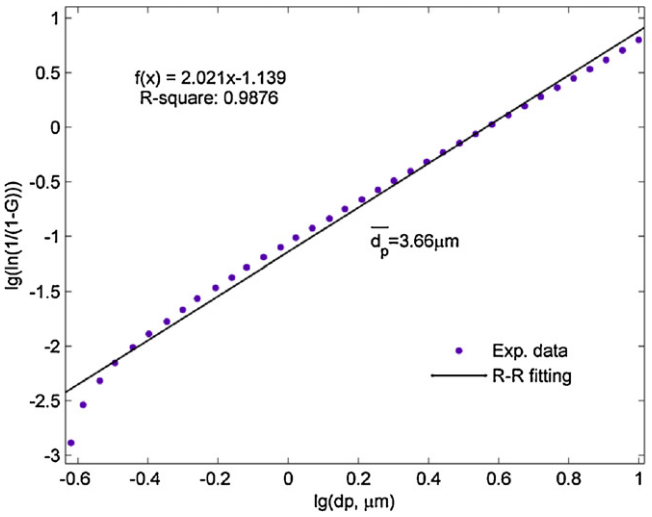

Fig. 2. Rosin–Rammler distribution of soot particles. G – the mass cumulative frequency; d_p – the particle size.

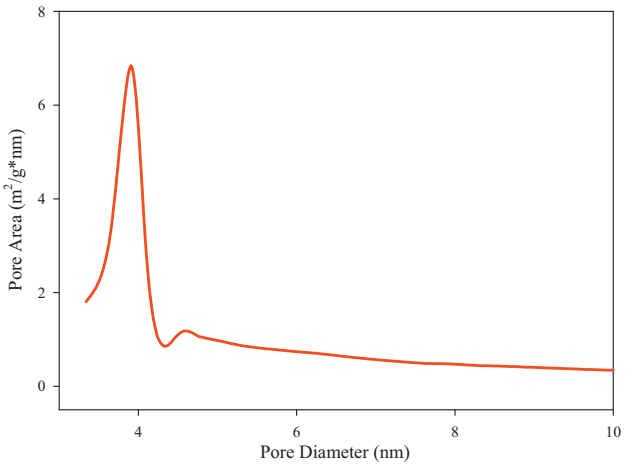

Fig. 3. Pore area distribution of soot particles.

in this study were much larger than those of previous reports [2,5,13,16,33]. This phenomenon could be the result of the soot particle agglomeration in the flue. It was reported [33] that when the particle was flied away from flame and then emitted into the flue, particle size distributions could be changed as a result of the coagulation of individual particles through collisions and adhesion. These processes would result in an increase in the average particle size.

The specific surface area and pore distribution of soot particles are also important physical properties. Because of the long atmospheric lifetimes of soot particles [16], their specific surface areas and pore volumes could significantly affect their adsorption properties and toxicity [7].

When the BET equation was employed to study the specific surface area, the BET surface area and pore volume resulted in a surface area of 14.589 m^2/g and a total pore volume of 0.0335 mL/g (P_s/P_o = 0.9814, N_2 adsorption). A plot of the pore area versus particle size is presented in Fig. 3. From Fig. 3 it is evident that most of the pore area resulted from pore diameters between 2 and 4 nm, indicating that pore diameters between 2 and 4 nm were the most abundant. The large pore volumes and number of nano-apertures indicated that soot particles could serve as adsorption surfaces for

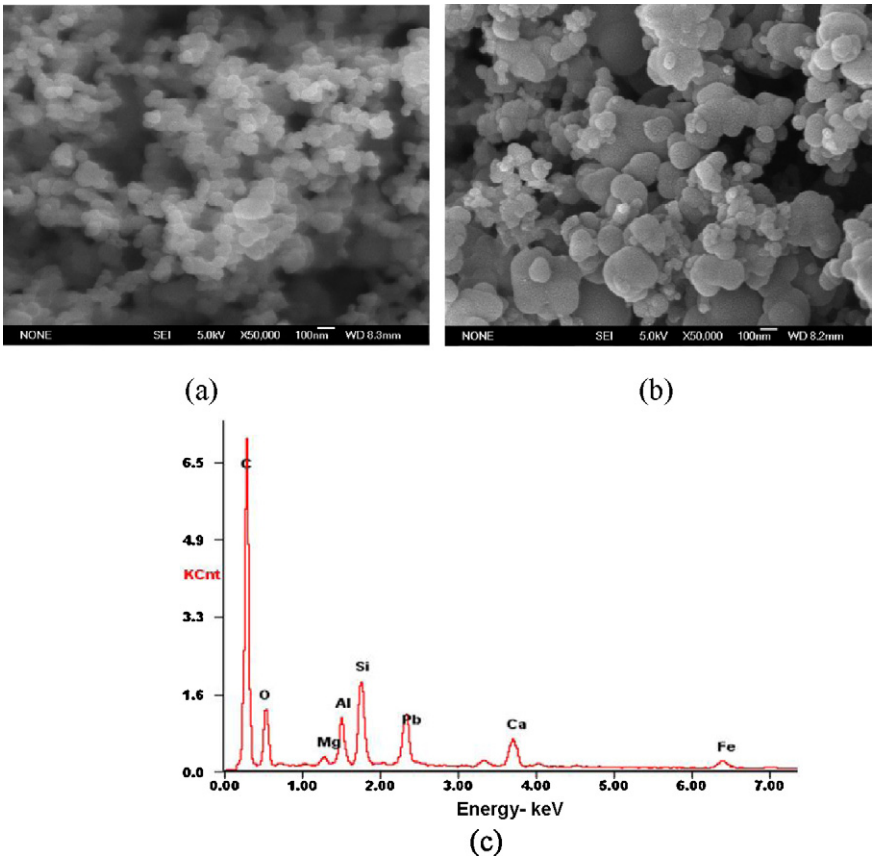

Fig. 4. (a and b) ESEM and (c) EDS of soot.

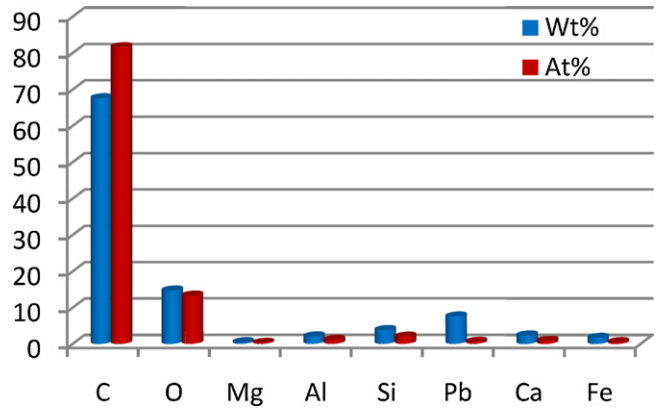

Fig. 5. Element compositions and its content of soot.

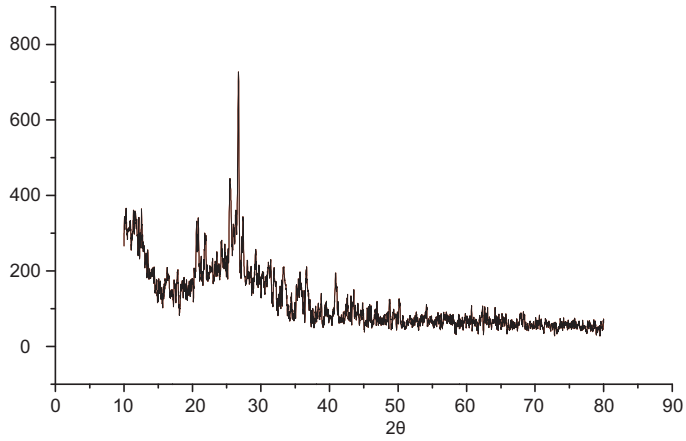

Fig. 6. XRD pattern of soot.

enriching harmful pollutants like PAHs upon entry into the atmosphere, or re-entrainment onto land or in water [5,13,19].

3.2. ESEM and EDS experiments

In order to visualize the pore diameters and surface features of the soot particles, ESEM and EDS experiments were performed. The results are presented in Fig. 4. Fig. 4(a) and (b) indicates that most soot particles were fine and smaller than 100 nm in diameter. The ESEM results also demonstrated that most of the fine particles appeared to be agglomerated, turning into larger particles. This gave the soot particles floc-like appearance and likely resulted in a measured particle size that was significantly greater than the actual particle size. The results presented in Fig. 4 also indicated that differences between the particle sizes in Figs. 1 and 2 and those reported previously were likely the result of soot particle agglomeration [17,33]. Kumar et al. [5,34] reported that particles emitted from bio-fuelled vehicles were <300 nm in size, while particles emitted from diesel vehicles were mainly distributed in the 10–300 nm range, with an overall size range of 10–2738 nm. Other work had reported that diesel soot and wood charcoal particles were, on average, less than 19 nm and larger than 10 μm, respectively [35,36]. Jiang et al. [13] also reported that particles emitted from diesel vehicles were less than 50 nm in diameter. The soot particle sizes in this study were significantly different from those reported, likely the results of the different fuel used and operating conditions. Differences in soot particle sizes for the combustion of coal were possible, since the combustion products might be different under different combustion conditions and with different types of coal. The reported particle sizes from coal combustion [37,38] were obviously different because the combustion conditions were significantly different from each other. Particle sizes in this study, slightly less than 100 nm, were similar to those obtained from transmission electron microscopy (JEM 3010, JEOL Ltd., Japan), shown in Fig. S1, and those reported by Ninomiya [38], which were obtained under similar combustion conditions.

The EDS experimental results are shown in Fig. 4(c), and the analysis of the results is presented in Fig. 5. In Figs. 4(c) and 5, it was evident that the soot particles were mostly carbonaceous. Many elements typical of atmospheric aerosols, like Si, Mg and Ca, were presented in the samples. Al was typically found in particles emitted from ceramic kilns. As reported previously [30], Pb was presented in the samples, potentially making the soot more toxic.

Using EDS, hydrogen has too low an atomic mass to be detected. When samples were analyzed using elemental analysis (Varop EIIII, ELEMENTAR Co., Germany), approximately 1.1% (w/w) H was detected, indicating the presence of organic compounds.

3.3. XRD experiment

In order to study the physical state of the elements detected in the EDS experiments, XRD studies of the soot samples were carried out. The powder XRD pattern of the soot sample is shown in Fig. 6.

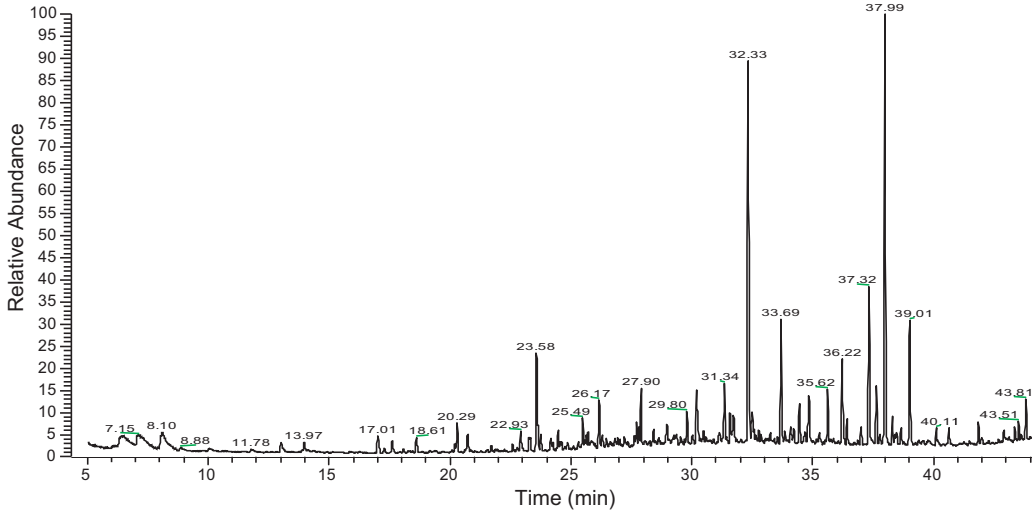

Fig. 7. GC/MS total ion chromatogram of organic pollutants in the soot samples.

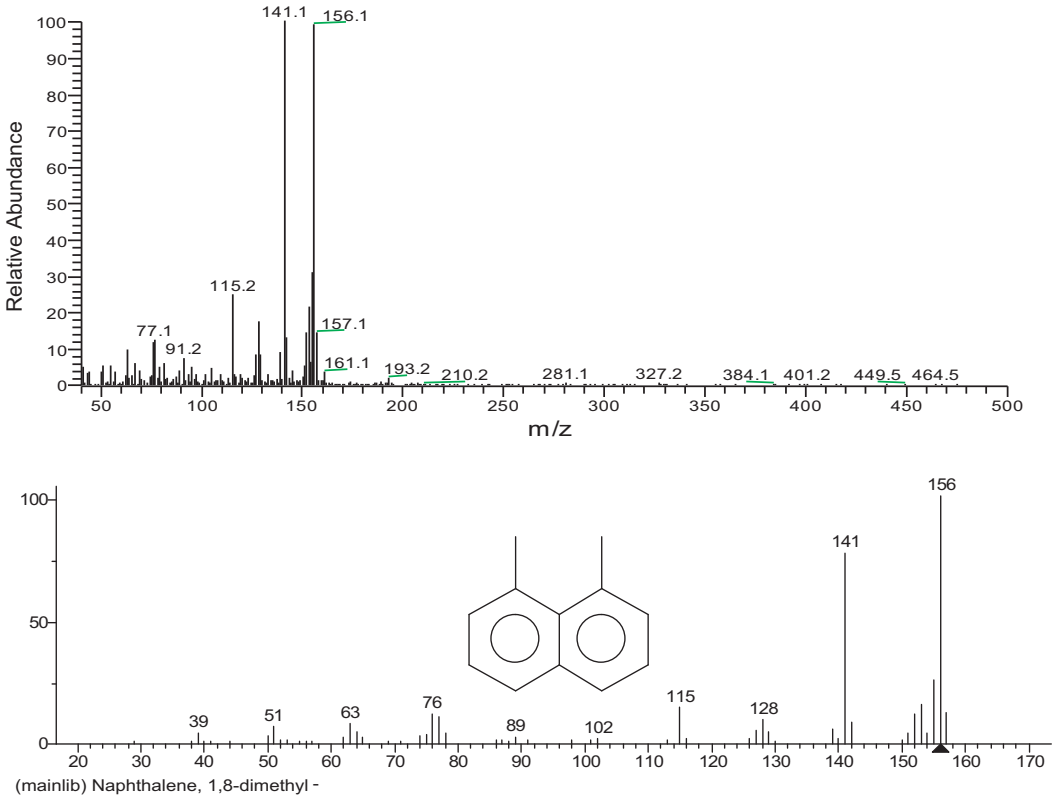

(a)

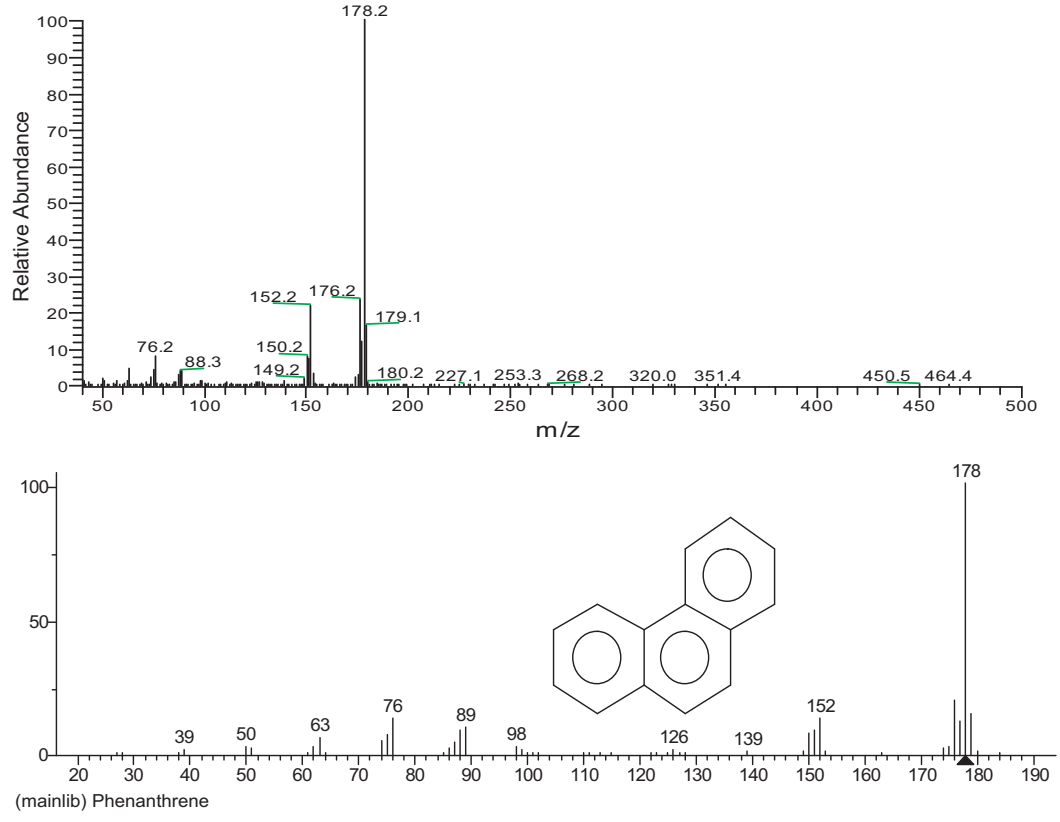

(b)

Fig. 8. Experimental and standard mass spectra of typical organic pollutants in soot. (a) 1,8-Dimethyl-naphthalene, (b) phenanthrene, (c) dibutylphthalate, (d) benzo[h]cinnoline, (e) 1,8-naphthalic anhydride, (f) cyclopenta[def]phenanthrene and (g) pyrene.

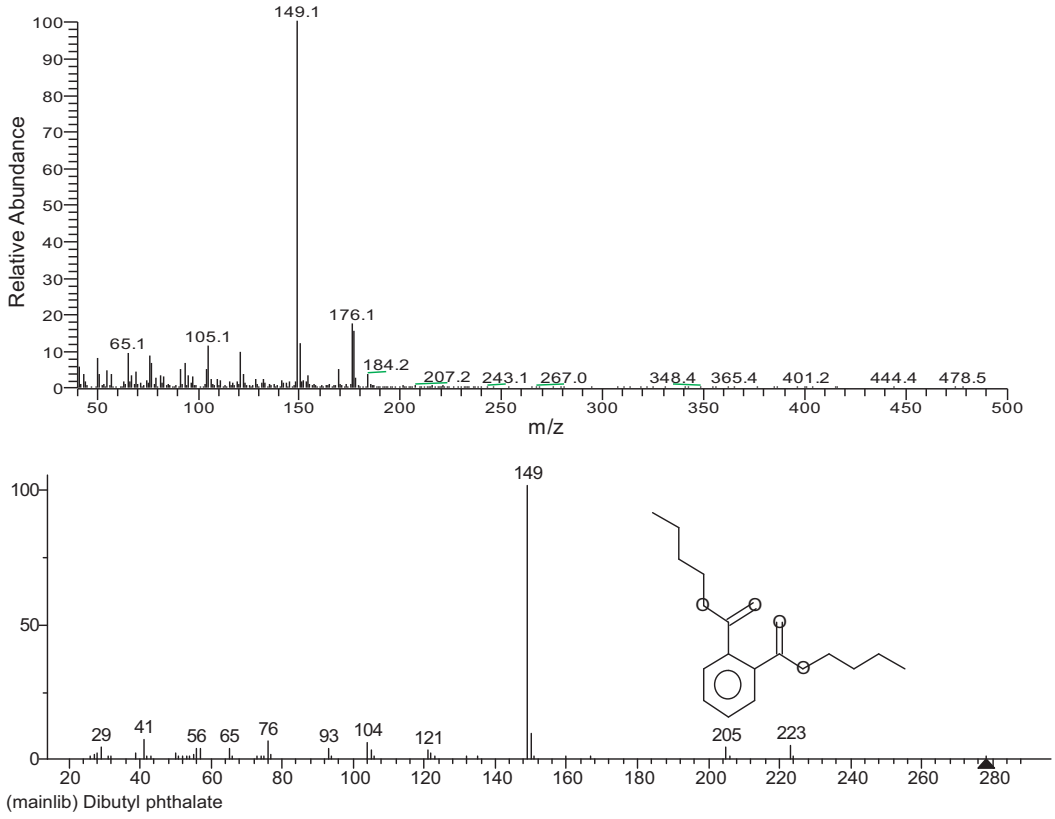

(c)

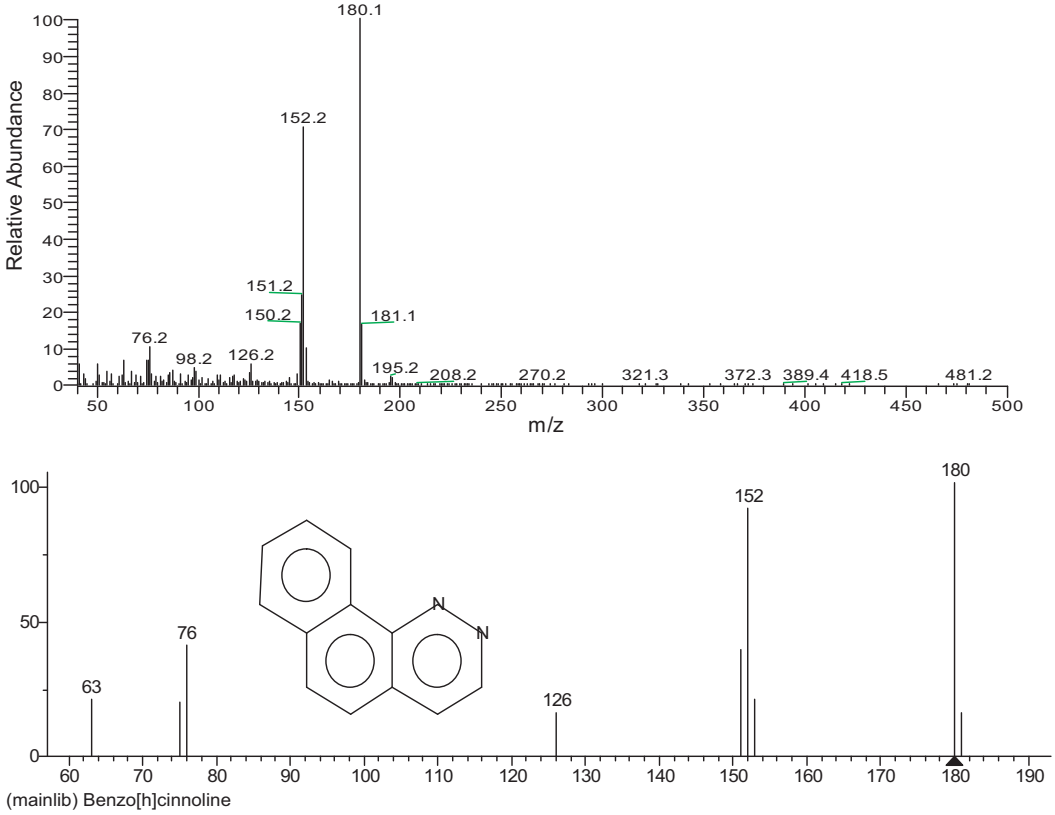

Fig. 8. *Continued*

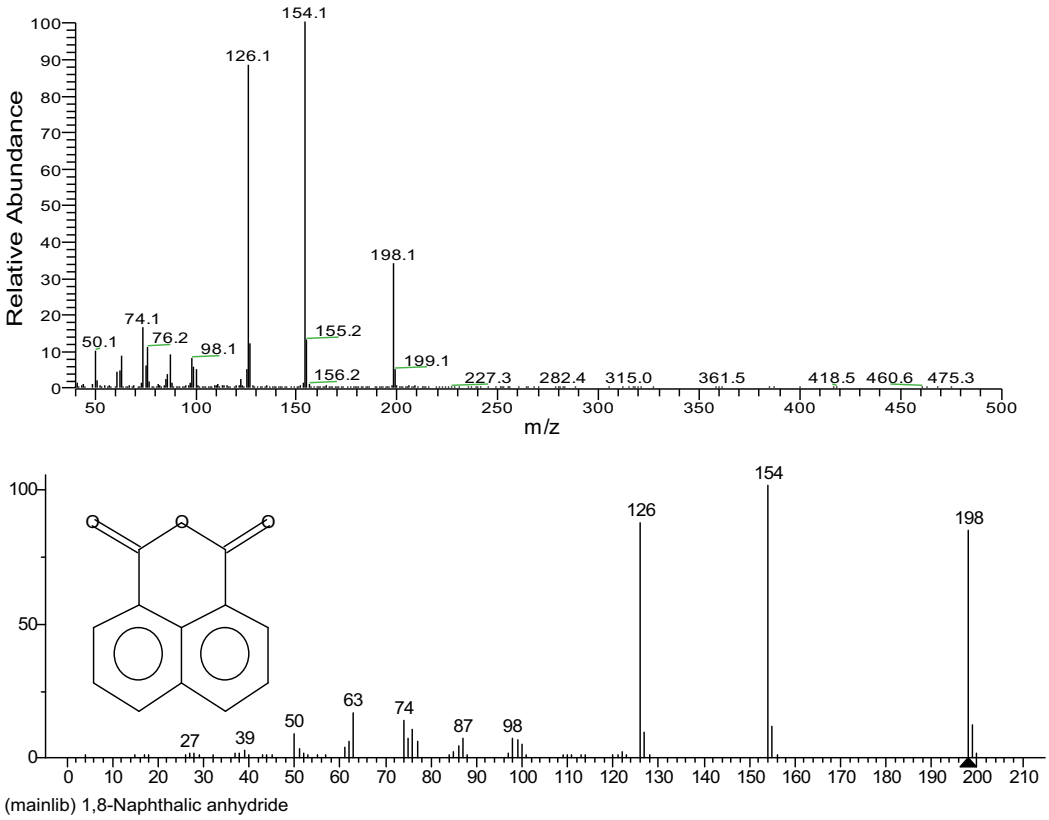

(e)

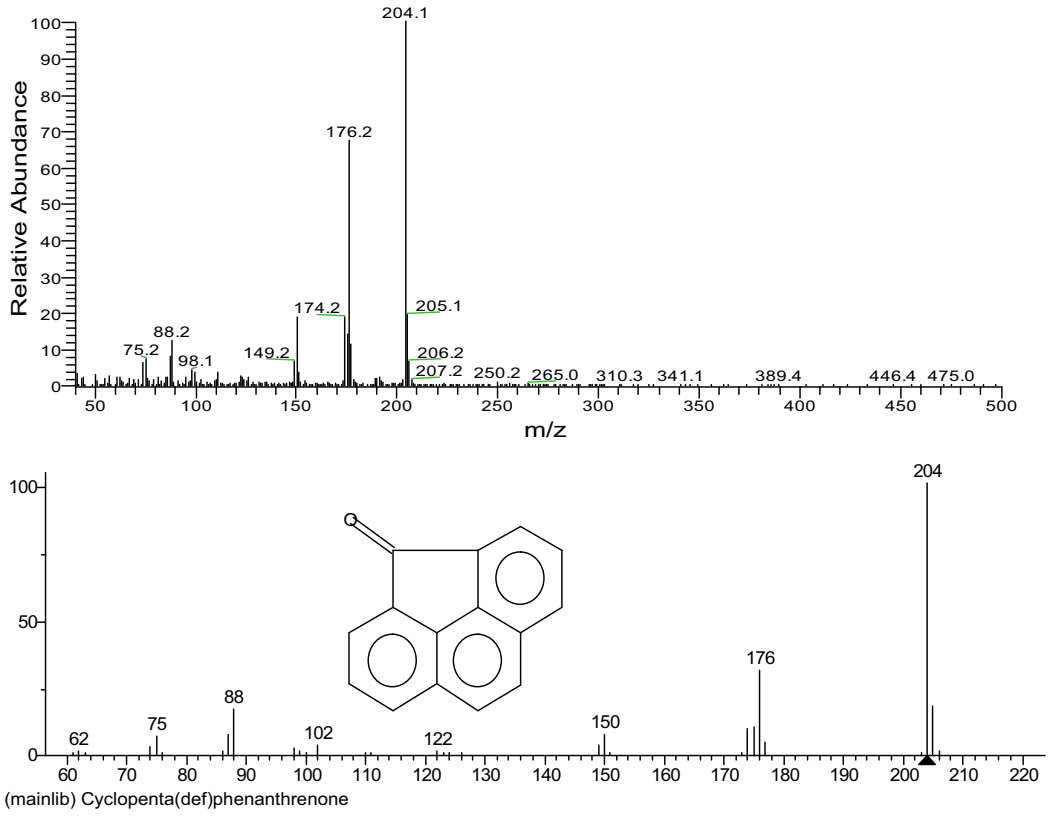

(f)

Fig. 8. *Continued*

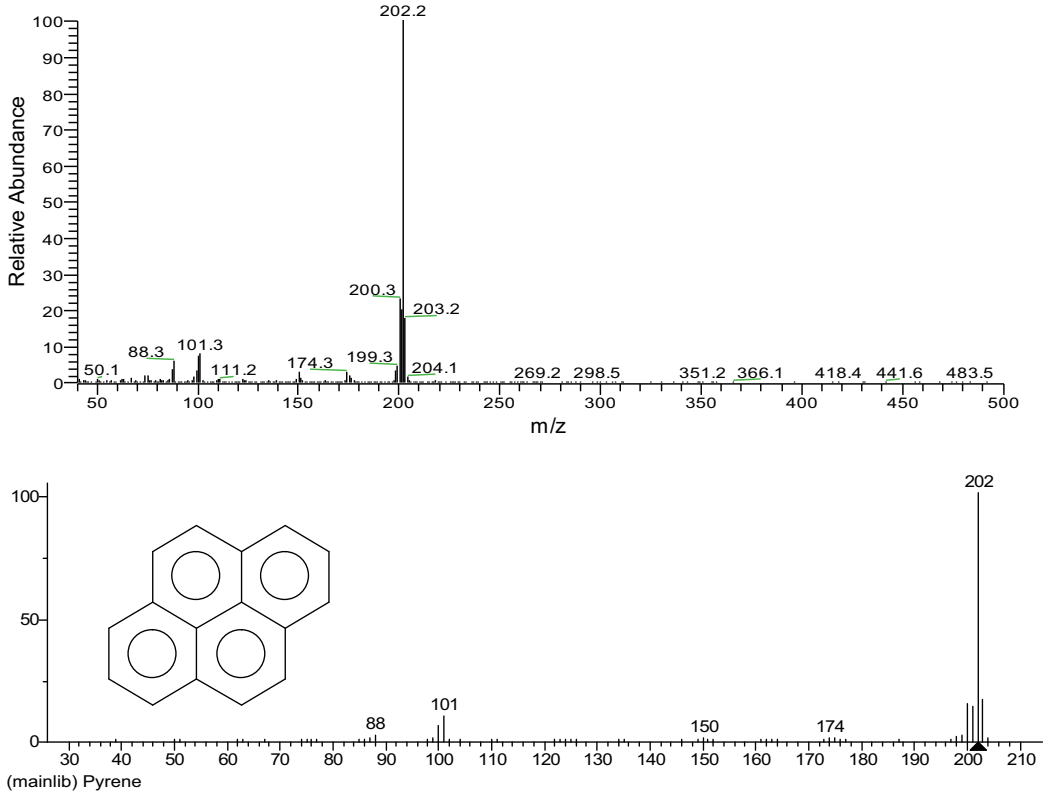

(g)

Fig. 8. *Continued*

The diffractogram in Fig. 6 was typical of amorphous carbon. There was no evidence of sharp Bragg peaks that could be attributed to mineral impurities in the carbon. The pattern did, however, show one broad feature at $2\theta = 24^{\circ}$, resulting from graphitic crystallites of carbon [39,40]. The location and broadness of the diffraction peak indicated that the soot sample had disordered carbonaceous inner layers [39]. There were no other obvious diffractograms from Fig. 6, indicating that there were no other crystallites in the soot, even with the many elements detected in Fig. 5. Since the metal elements detected in EDS experiments were in amorphous status, their shapes and light-scattering properties could be changed, especially when they floated in the air (NASA, website: http://www.nasa.gov/topics/earth/features/cares-cali.html). If this phenomenon occurred, soot particles would result in significantly negative impact on climate. Meanwhile, with soot particles adsorbing pollutants from the surroundings, they could cause more harms. Therefore, the soot with these hazardous organic pollutants might turn into more harmful pollutants through a series of chemical reactions under some atmospheric condition.

3.4. GC/MS

Organic pollutants like PAHs and volatile organic compounds are well-known to be presented in soot and other particles [13,18,19,33,41]. In order to study the organic component composition of the soot samples, GC/MS analyses were carried out. The GC/MS total ion chromatograms of organic species presented in the soot samples were analyzed and a typical chromatogram is shown in Fig. 7.

Qualitative assessments of the chromatograms revealed approximately 90 different organic species in the samples. The following five categories of organic pollutants were characterized:

(1) pollutants generated by the incomplete combustion of coal, such as 2-hexyl alcohol, p-cresol and 2-hydroxyacetophenone;
(2) acidic oxides generated by silylation;
(3) hydroxybenzene;
(4) PAHs; and
(5) other organic pollutants, such as alkanes.

Among the 90 different organic species, seven typical organic species are presented in Fig. 8(a)–(g) with their mass spectra, names and chemical structures. The residence times, peak areas and percentages of the seven species are provided in Table S1. The percentages were calculated using the area normalization method.

Previous studies have reported similar GC/MS results for nanoparticles emitted from bio-fuel vehicles, elemental carbon particles, black carbon from fly ash and soot [5,13,18–20,24,33,41]. These reports suggested that the organic species presented in Fig. 8 were harmful organic pollutants in soot. With sustained accumulation, 1,8-dimethyl-naphthalene (Fig. 8(a)) [42–45], phenanthrene (Fig. 8(b)), benzo[h]cinnoline (Fig. 8(d)), 1,8-naphthalic anhydride (Fig. 8(e)), cyclopenta[def]phenanthrenone (Fig. 8(f)) and pyrene (Fig. 8(g)) can not only seriously pollute the environment but also significantly affect human health [46,47]. For example, these compounds are known, or suspected to cause leukemia and other cancers [48,49], particularly phenanthrene and pyrene [19,42,45]. Dibutylphthalate (Fig. 8(c)) has high chemical, biochemical and physical stability, and is classified as a persistent pollutant. Because of its persistence and lipophilic characteristics, dibutylphthalate can be adsorbed to soot particles and accumulated in soils, sediments and plants [13,47]. Table S1 shows that phenanthrene, 1,8-naphthalic anhydride and pyrene were the most abundant of the seven pollutant species characterized. Though the concentration of dibutylphthalate, which made up 0.94% of the organic pollutants detected in the soot particles, was lower than that of

most of the selected organic pollutants, it is likely one of the most hazardous compounds because of its strong chemical and physical stability. Dibutylphthalate has been observed in the food chain and human breast milk [18,19,42,45–47,50]. Furthermore, other hydrocarbon pollutants just like aromatic compounds were also carcinogenic. Alkanes detected in the soot could damage environment by forming photochemical smog.

4. Conclusions

The soot samples studied in this paper were nanoparticles, with diameter smaller than 100 nm. These particles tended to agglomerate into larger particles with median diameter of 3.66 μm. Various organic pollutants, like aromatic carcinogenic compounds, as well as heavy metals were presented in the soot. Many elements were presented in the soot samples, but they existed in an amorphous state. The soot particles had large BET surface areas and pore diameters, making them good adsorption surfaces for other pollutants, like hydrocarbons. Because of this, the particles could evolve into more hazardous atmospheric pollutants when they were emitted into the atmosphere. Because of less concern about soot pollution from ceramic furnace flue gas, controlling emissions from this source is very important. Given the chemical and physical properties of the soot particles, some commonly used dust purification methods, such as bag filter and electrostatic precipitation, are not applicable to the removal of soot from BS. Wet de-dusting with a suitable absorbent, like a surfactant solution, is a desirable and convenient method for removing soot from the BS of a stationary source. This will be the focus of our further study.

Acknowledgements

This work was supported by the National Natural Science Foundation of China (Nos. 50878080, 51108169, and 50908080), the National High Technology Research and Development Program of China (863 Program, No. 2011AA060803), the Scientific and Technological Major Special Project of Changsha City in China (No. K0902006-31), the Scientific and Technological Major Special Project of Hunan Province in China (No. 2010XK6003), the Scientific and Technological Project of Hunan Province in China (No. 2011SK3219), the Fundamental Research Funds for the Central Universities. The authors thank Prof. Chenggang Niu (Hunan University, China), Dr. Li-meimei Xu (Illinois Institute of Technology, USA) and Yide He (Humboldt University, Germany) for their help with this study.

Appendix A. Supplementary data

Supplementary data associated with this article can be found, in the online version, at doi:10.1016/j.jhazmat.2011.11.004.

References

[1] Y. He, G.L. Zhang, Historical record of black carbon in urban soils and its environmental implications, Environ. Pollut. 157 (2009) 2684–2688.
[2] P. Kumar, M. Ketzel, S. Vardoulakis, L. Pirjola, R. Britter, Dynamics and dispersion modelling of nanoparticles from road traffic in the urban atmospheric environment – a review, J. Aerosol Sci. 42 (2011) 580–603.
[3] A.S. Panicker, G. Pandithurai, P.D. Safai, S. Dipu, D.-I. Lee, On the contribution of black carbon to the composite aerosol radiative forcing over an urban environment, Atmos. Environ. 44 (2010) 3066–3070.
[4] K. Gowdy, Q.T. Krantz, M. Daniels, W.P. Linak, I. Jaspers, M.I. Gilmour, Modulation of pulmonary inflammatory responses and antimicrobial defenses in mice exposed to diesel exhaust, Toxicol. Appl. Pharmacol. 229 (2008) 310–319.
[5] P. Kumar, A. Robins, H. ApSimon, Nanoparticle emissions from biofuelled vehicles – their characteristics and impact on the number-based regulation of atmospheric particles, Atmos. Sci. Lett. 11 (2010) 327–331.
[6] D. Goto, T. Takemura, T. Nakajima, K.V.S. Badarinath, Global aerosol model-derived black carbon concentration and single scattering albedo over Indian region and its comparison with ground observations, Atmos. Environ. 45 (2011) 3277–3285.
[7] J.F. Mejía, S.L. Choy, K. Mengersen, L. Moreawska, Methodology for assessing exposure and impacts of air pollutants in school children: data collection analysis and health effects – a literature review, Atmos. Environ. 45 (2011) 813–823.
[8] H. Inouea, A. Shimada, T. Kaewamatawong, M. Naota, T. Morita, Y. Ohta, K. Inoue, H. Takano, Ultra structural changes of the air–blood barrier in mice after intratracheal instillation of lipopolysaccharide and ultrafine black carbon particles, Exp. Toxicol. Pathol. 61 (2009) 51–58.
[9] V.A. Dutkiewicz, S. Alvi, B.M. Ghauri, M.I. Choudhary, L.T. Husain, Black carbon aerosols in urban air in South Asia, Atmos. Environ. 43 (2009) 1737–1744.
[10] T. Ahmed, V.A. Dutkiewicz, A. Shareef, G. Tuncel, S. Tuncel, L. Husain, Measurement of black carbon (BC) by an optical method and a thermal–optical method intercomparison for four sites, Atmos. Environ. 43 (2009) 6305–6311.
[11] K.R. Kumar, K. Narasimhulu, G. Balakrishnaiah, B.S.K. Reddy, K.R. Gopal, R.R. Reddy, S.K. Satheesh, K.K. Moorthy, S.S. Babu, Characterization of aerosol black carbon over a tropical semi-arid region of Anantapur, India, Atmos. Res. 100 (2011) 12–27.
[12] T. Novakova, J.E. Hansen, Black carbon emissions in the United Kingdom during the past four decades: an empirical analysis, Atmos. Environ. 38 (2004) 4155–4163.
[13] M.Y. Jiang, J.Q. Li, Y.Q. Wu, N.T. Lin, X.M. Wang, F.F. Fu, Chemical characterization of nanometer-sized elemental carbon particles emitted from diesel vehicles, J. Aerosol Sci. 42 (2011) 365–371.
[14] N. Riemer, M. West, R. Zaveri, R. Easter, Estimating black carbon aging timescales with a particle-resolved aerosol model, J. Aerosol Sci. 41 (2010) 143–158.
[15] E. Uherek, T. Halenka, J.B. Kleefeld, Y. Balkanski, T. Berntsen, C. Borrego, M. Gauss, P. Hoor, K.J. Rezler, J. Lelieveld, D. Melas, K. Rypdal, S. Schmid, Transport impacts on atmosphere and climate: land transport, Atmos. Environ. 44 (2010) 4772–4816.
[16] U.C. Dumka, K.K. Moorthy, R. Kumar, P. Hegde, R. Sagar, P. Pant, N. Singh, S.S. Babu, Characteristics of aerosol black carbon mass concentration over a high altitude location in the Central Himalayas from multi-year measurements, Atmos. Res. 96 (2010) 510–521.
[17] X. Cui, C.T. Li, F. Wang, S.M. Li, C. Xiao, Y. Peng, Y.B. Zhai, Experimental study on the control of black smoke pollution from the ceramic kilns based on the mechanism of the surfactant and coagulant, Front. Environ. Sci. Eng. China 2 (2007) 109–115.
[18] P.J. Tsai, H.Y. Shieh, W.J. Lee, S.O. Lai, Characterization of PAHs in the atmosphere of carbon black manufacturing workplaces, J. Hazard. Mater. A91 (2002) 25–42.
[19] L. Lou, L. Luo, W. Wang, X. Xu, J. Hou, B. Xun, Y. Chen, Impact of black carbon originated from fly ash and soot on the toxicity of pentachlorophenol in sediment, J. Hazard. Mater. 190 (2011) 474–479.
[20] F. Yang, Y. Zhai, L. Chen, C. Li, G. Zeng, Y. He, Z. Fu, W. Peng, The seasonal changes and spatial trends of particle-associated polycyclic aromatic hydrocarbons in the summer and autumn in Changsha city, Atmos. Res. 96 (2010) 122–130.
[21] IPCC, in: S. Solomon, D. Qin, M. Manning, Z. Chen, M. Marquis, K.B. Averyt, M. Tignor, H.L. Miller (Eds.), Contribution of Working Group I to the Fourth Assessment Report of the Intergovernmental Panel on Climate Change, Cambridge University Press, Cambridge, United Kingdom/New York, NY, USA, 2007, p. 996.
[22] S. Menon, J. Hansen, L. Nazarenko, Y. Luo, Climate effects of black carbon aerosols in China and India, Science 297 (2002) 2250–2253.
[23] X. Zhou, J. Gao, T. Wang, W. Wu, W. Wang, Measurement of black carbon aerosols near two Chinese megacities and the implications for improving emission inventories, Atmos. Environ. 43 (2009) 3918–3924.
[24] J. Cheng, T. Yuan, Q. Wu, W. Zhao, H. Xie, Y. Ma, J. Ma, W. Wang, PM_{10}-bound polycyclic aromatic hydrocarbons (PAHs) and cancer risk estimation in the atmosphere surrounding an industrial area of Shanghai, China, Water Air Soil Pollut. 183 (2007) 437–446.
[25] P.J. Brochu, M.A. Kioumourtzoglou, B.A. Coull, P.K. Hopke, H.H. Suh, Development of a new method to estimate the regional and local contributions to black carbon, Atmos. Environ. (2011), doi:10.1016/j.atmosenv.2011.01.074.
[26] L. Wang, C. Jang, Y. Zhang, K. Wang, Q. Zhang, D. Streets, J. Fu, Y. Lei, J. Schreifels, K. He, J. Hao, Y. Lam, J.L.N. Meskhidze, S. Voorhees, D. Evarts, S. Phillips, Assessment of air quality benefits from national air pollution control policies in China. Part I: background emission scenarios and evaluation of meteorological predictions, Atmos. Environ. 44 (2010) 3442–3448.
[27] J.C. Chow, J.G. Watson, P. Doraiswamy, L.W.A. Chen, D.A. Sodeman, D.H. Lowenthal, K. Park, W.P. Arnott, N. Motallebi, Aerosol light absorption, black carbon, and elemental carbon at the Fresno Supersite, California, Atmos. Res. 93 (2009) 874–887.
[28] S. Koga, T. Maeda, N. Kaneyasu, Source contributions to black carbon mass fractions in aerosol particles over the northwestern Pacific, Atmos. Environ. 42 (2008) 800–814.
[29] P. Lu, C.T. Li, G.M. Zeng, L.J. He, D.L. Peng, H.F. Cui, S.H. Li, Y.B. Zhai, Low temperature selective catalytic reduction of NO by activated carbon fiber loading lanthanum oxide and ceria, Appl. Catal. B: Environ. 96 (2010) 157–161.
[30] V. Mugica, M. Maubert, M. Torres, J. Munoz, E. Rico, Temporal and spatial variations of metal content in TSP and PM10 in Mexico City during 1996–1998, J. Aerosol Sci. 33 (2002) 91–102.
[31] A.M. García, E.M. Cuerda-Correab, M.A. Díaz-Díez, Application of the Rosin–Rammler and Gates–Gaudin–Schuhmann models to the particle size distribution analysis of agglomerated cork, Mater. Charact. 52 (2004) 159–164.
[32] W. Zhang, C.T. Li, X. Wei, H.L. Gao, Q.B. Wen, X.P. Fan, X. Shu, G.M. Zeng, W. Wei, Y.B. Zhai, Y.D. He, S.H. Li, Effects of cake collapse caused by deposition of fractal

aggregates on pressure drop during ceramic filtration, Environ. Sci. Technol. 45 (2011) 4415–4421.
[33] K.M. Butler, G.W. Mulholland, Generation and transport of smoke components, Fire Technol. 40 (2004) 149–176.
[34] P. Kumar, P. Fennell, D. Langley, R. Britter, Pseudo-simultaneous measurements for the vertical variation of coarse fine and ultra fine particles in an urban street canyon, Atmos. Environ. 42 (2008) 4304–4319.
[35] E. Ghzaoui, M. Lindheimer, A. Lindheimer, S. Lagerge, S. Partyka, Surface characterization of diesel engine soot inferred from physico-chemical methods, Colloids Surf. A: Physicochem. Eng. Aspects 233 (2004) 79–86.
[36] F. Thevenon, F.S. Anselmetti, Charcoal and fly-ash particles from Lake Lucerne sediments (Central Switzerland) characterized by image analysis: anthropologic. stratigraphic and environmental implications, Quaternary Sci. Rev. 26 (2007) 2631–2643.
[37] F. Carbone, F. Beretta, A. D'Anna, Multimodal ultrafine particles from pulverized coal combustion in a laboratory scale reactor, Combust. Flame 157 (2010) 1290–1297.
[38] Y. Ninomiya, L. Zhang, A. Sato, Z.B. Dong, Influence of coal particle size on particulate matter emission and its chemical species produced during coal combustion, Fuel Process. Technol. 85 (2004) 1065–1088.
[39] D. Borah, S. Satokawa, S. Kato, T. Kojima, Characterization of chemically modified carbon black for sorption application, Appl. Surf. Sci. 254 (2008) 3049–3056.
[40] V.S. Badu, M.S. Seehra, Modeling of disorder and X-ray diffraction in coal-based graphitic carbons, Carbon 34 (1996) 1259–1265.
[41] E.M. Fitzpatrick, A.B. Ross, J. Bates, G. Andrews, J.M. Jones, H. Phylaktou, M. Pourkashanian, A. Williams, Emission of oxygenated species from the combustion of pine wood and its relation to soot formation, Process Saf. Environ. 85 (2007) 430–440.
[42] D. Cao, Z. Wang, C. Han, L. Cui, Mi. Hu, J. Wu, Y. Liu, Y. Cai, H. Wang, Y. Kang, Quantitative detection of trace perfluorinated compounds in environmental water samples by Matrix-assisted Laser Desorption/Ionization-Time of Flight Mass Spectrometry with 1,8-bis(tetramethylguanidino)-naphthalene as matrix, Talanta 85 (2011) 345–352.
[43] C.Y. Lin, Å.M. Wheelock, D. Morin, R.M. Baldwin, M.G. Lee, A. Taff, C.P.A. Buckpitt, A. Rohde, Toxicity and metabolism of methylnaphthalenes: comparison with naphthalene and 1-nitronaphthalene, Toxicology 260 (2009) 16–27.
[44] J.C. Tsai, M. Kumar, J.G. Lin, Anaerobic biotransformation of fluorene and phenanthrene by sulfate-reducing bacteria and identification of biotransformation pathway, J. Hazard. Mater. 164 (2009) 847–855.
[45] C. Yan, Y. Yang, M. Liu, M. Nie, J.L. Zhou, Phenanthrene sorption to Chinese coal: importance of coal's geochemical properties, J. Hazard. Mater. 192 (2011) 86–92.
[46] I. Sýkorová, M. Havelcová, H. Trejtnarová, P. Matysová, M. Vašíček, B. Kříbek, V. Suchý, B. Kotlík, Characterization of organic matter in dusts and fluvial sediments from exposed areas of downtown Prague, Czech Republic, Int. J. Coal Geol. 80 (2009) 69–86.
[47] D. Apic, F. Bonner, B. Cosovic, R.B. Russell, Genes from liver tissue affected in phthalate treated rats coupled with structural analysis of phthalates jointly predict testicular toxicity and elucidates possible mechanisms, Toxicology 278 (2010) 341–378.
[48] Z. Li, Y. Wu, Y. Zhao, L. Wang, H. Zhu, L. Qin, F. Feng, W. Wang, Y. Wu, Analysis of coal tar pitch and smoke extract components and their cytotoxicity on human bronchial epithelial cells, J. Hazard. Mater. 186 (2011) 1277–1282.
[49] K. Mäenpää, M.T. Leppänen, J.V.K. Kukkonen, Sublethal toxicity and biotransformation of pyrene in *Lumbriculus variegatus* (Oligochaeta), Sci. Total Environ. 407 (2009) 2666–2672.
[50] J. Koistinen, J. Paasivirta, M. Suonpera, H. Hyvarinen, Contamination of pike and sediment from the Kymijoki River by PCDEs PCDDs, and PCDFs: contents and patterns compared to pike and sediment from the Bothnian Bay and seals from Lake Saimaa, Environ. Sci. Technol. 29 (1995) 2541–2547.